Chemical Process Design Vol.4 No.2 (2025) 38-49

University of Sistan and Baluchestan

Chemical Process Design

Available online at http://cpd.usb.ac.ir/

Effective Acetylation of Hydroxyl Compound with $Ru^{III}(OTf)_2$ Salen Modified SiO_2–Fe_3O_4 Magnetically Recycling Catalyst

Somayeh Mehdigholami[1]✉, Esmaeil Koohestanian[2]

[1] Corresponding Author, Shahid Ahmadi Roshan Research Center, Abadeh, Fars, Iran. E-mail: mehdigholami@grad.kashanu.ac.ir
[2] Department of Chemical Engineering, Islamic Azad University, Iranshahr Branch, Iranshahr, Iran. E-mail: koohestanian@pgs.usb.ac.ir

ARTICLE INFO

Article type:
Research Article

Article history:
Received: 2025-04-01
Received in revised form: 2025-08-02
Accepted: 2025-08-03
Available online: 2025-08-03

Keywords: *Magnetic nanoparticles; Salen Ru(OTf)₂; Acetylation; Alcohol acetylation; Phenol acetylation; Schiff base; Recyclable Nano catalyst*

ABSTRACT

This study reports the successful synthesis of $Ru(OTf)_2$ immobilized on an amino-functionalized Schiff base-modified SiO_2–Fe_3O_4 magnetic nanocomposite, which serves as an efficient and rapidly recyclable catalyst for the acetylation of primary alcohols and phenols. The Fe_3O_4_SiO_2/Schiff-base/Ru(III) magnetic nanoparticles were thoroughly characterized by Fourier Transform Infrared Spectroscopy (FT-IR), X-ray Diffraction (XRD), UV-visible spectroscopy (UV-Vis), Scanning Electron Microscopy (SEM), Energy-Dispersive X-ray (EDX) analysis, and Vibrating Sample Magnetometry (VSM). Notably, the use of only 0.1 mmol of catalyst with acetic anhydride provided excellent acetylation efficiency. The acetylation of alcohols and phenols with acetic anhydride afforded the desired acetates in 87–93% yield within 3–9 minutes. Furthermore, the catalyst could be easily recovered using an external magnet and reused multiple times without significant loss of catalytic performance, highlighting its potential for green and sustainable chemistry.

Cite this article: Mehdigholami, S., Koohestanian, E., (2025), Effective Acetylation of Hydroxyl Compound with $Ru^{III}(OTf)_2$ Salen Modified SiO_2–Fe_3O_4 Magnetically Recycling Catalyst, *Chemical Process Design*, 4(2), 38-49. http//doi.org/10.22111/cpd.2025.50678.1053

© The Author(s).
DOI: http//doi.org/10.22111/cpd.2025.50678.1053

Publisher: University of Sistan and Baluchestan.

1. Introduction

The advancement of eco-friendly technologies for producing high quality chemicals product is a considerable concern for chemists specifying in synthetic chemistry. From this perspective, the development of metal catalysts and reagents that are bound to polymers and offer enhanced usefulness and selectivity has garnered substantial interest [1]. The protection of hydroxyl groups is frequently essential in the development of synthesizing refined compounds and organic substances [2-3]. Different techniques have been documented for the protection of hydroxyl groups, involving acetylation, tetrahydropyranylation, methoxymethylation, and trimethylsilylation [4,5]. Acetylation is a vital technique in the organic synthesis, as acetate ester groups can effectively protect a diverse range of functional groups

such as alcohols, phenols, amines, and thiols. This can be achieved using acetyl chloride [6-8] and acetic anhydride [9-11], that are usually utilized as the acylating agents, in the presence of suitable homogeneous or heterogeneous acid catalysts or base catalysts. Various catalytic systems have been studied for the esterification of alcohols with acetic anhydride, such as metal-based Lewis acids [7] and metal triflates [12]. Additionally, a range of homogeneous or heterogeneous catalysts, including ($ZnAl_2O_4$) [13], poly (4-vinylpyridinium) perchlorate [14], $ZnAl_2O_4$_ SiO_2 nanocomposite [15], and Molybdenum-modified mesoporous SiO_2, have been employed for this reaction [16]. Metal Schiff base complexes are commonly acknowledged in the field of coordination chemistry, primarily due to their stability, ease of synthesis, structural flexibility, and diverse range of applications [17]. Salen and Salophen ligands, containing nitrogen and oxygen donor atoms [18], are significant catalysts in numerous organic reactions. Complexes of Ruthenium have advantageous properties as electron transfer agents and are employed as oxidation catalysts [19-20], for studying biological macromolecules [21], and in organic synthesis [22-23]. The Metal Schiff base complex nanoparticles can be immobilized on the surface of Fe_3O_4_SiO_2 to enhance their stability against air and heat. This immobilization not only enhances thermal and air stability but also improves efficiency by utilizing the high surface-to-volume ratio [24].

Schiff bases are highly esteemed as ligands for Ru complexes due to several factors. Firstly, the steric and electronic properties in the vicinity of the ruthenium nucleus can be precisely adjusted by modifying the substituents in the Schiff bases. Furthermore, in chelated Schiff bases, the two donor atoms—nitrogen and oxygen—exhibit contrasting electronic effects: the phenolate oxygen functions as a hard donor, stabilizing the higher oxidation state of the ruthenium atom, while the imine nitrogen serves as a softer donor, stabilizing the lower oxidation state. Lastly, Schiff bases can be readily synthesized through simple condensation methods that involve combining easily accessible aldehydes with amines, resulting in high yields [25].

The ability to reuse catalysts is a crucial consideration in various catalytic processes in heterogeneous systems, where recovery techniques like centrifugation or filtration are used [26]. Nanoparticles have garnered important attention in catalysis due to their greater specific surface area compared to bulk materials. However, recovering these small particles from the reaction medium poses challenges [27]. In response to this issue, magnetic nanoparticles have emerged as a promising solution. Their paramagnetic properties facilitate easy and efficient recovery using an external magnet, allowing for reuse in subsequent cycles [28]. Magnetic Nano catalysts have been utilized in a wide array of reactions with effective activities and can undergo surface-functionalization during the catalyst preparation process [29-30].

Following the observing the impressive catalytic performance of Fe_3O_4_SiO_2/Schiff-base/Ru MNPs, we introduced a Salen Schiff-based Nano catalyst. This research aims to synthesize, analyze, and investigate the catalytic efficiency of these nanoparticles for acetylating hydroxyl compounds. This method achieves complete conversion of substrates with exceptional catalyst retrieval at relatively low reaction temperatures in an air environment. The optimized reaction parameters are then utilized to produce a range of acetylated derivatives with remarkably high yields.

The present work introduces a novel magnetic Nano catalyst system based on $Ru(III)(OTf)_2$ Salen complexes immobilized on amino-functionalized Schiff base-modified SiO_2–Fe_3O_4 nanoparticles.. Compared to previously reported catalysts, this system stands out due to its truly nanoscale dimensions, which provide a significantly higher surface area and enhanced catalytic efficiency. The uniform and well-dispersed morphology, as confirmed by SEM analysis, ensures optimal accessibility of active sites. Moreover, the superparamagnetic properties of the catalyst

enable rapid and straightforward magnetic separation and recycling, addressing a key challenge in heterogeneous catalysis. This innovative approach combines the high activity and selectivity of Ru(III) Salen complexes with the practical advantages of magnetic nanotechnology, leading to excellent yields (87–93%) in the acetylation of alcohols and phenols within remarkably short reaction times (3–9 minutes) under mild conditions. The catalyst's robust reusability, along with its green and sustainable features, marks a significant advancement over conventional systems and highlights its great potential for practical and industrial applications.

2. Experimental

2.1. Material and method

All chemical materials employed in this research were obtained from Sigma-Aldrich (USA) and Merck (Germany) company. The phase and crystalline structure of the magnetic nanoparticles (MNPs) were studied by X-ray Diffraction (XRD) with a Bruker AXS D8-Advance diffractometer, utilizing Cu-Kα radiation (λ = 1.5418 Å) over a 2θ range of 10 to 80 degrees. The Fourier Transform Infrared Spectroscopy (FT-IR) spectra (JASCO 6300 spectrophotometer). The nitrogen content was measured via CHNS analysis by a Leco 932 instrument. The diffuse-reflectance UV–visible spectrum was taken with a JASCO V-670 solid UV–visible spectrophotometer. Scanning Electron Microscopy (SEM) images were taken using a TESCAN microscope. Elemental characterization of the materials was carried out using Energy-dispersive X-ray (EDX) analysis. The magnetization of the nanoparticles (NPs) was measured using the Vibrating Sample Magnetometer (VSM) technique. Additionally, experiments were performed using a Shimadzu GC-16A instrument, which was fitted with either a 2-meter column packed with silicon DC-200 or a 20-meter Carbowax column.

This work estimated the catalytic activity using turnover frequency (TOF) values, which are estimated as TOF = TON/reaction time. The turnover number (TON) shows the moles of reactant utilized per mole of catalyst. TOF determinations were achieved using Eqs. (1) and (2) [33]. The TOF of the catalyst is summarized in Table 4.

$$\text{TON} = \text{mole product achieved/ mole catalyst} \quad (1)$$

$$\text{TOF } (h^{-1}) = \text{TON/reaction time (h)} \quad (2)$$

22.2 Synthesis of Fe_3O_4 Nanoparticles

Magnetic iron oxide nanoparticles were synthesized using the co-precipitation method. In this method, under an argon atmosphere, 8.5 g (31.45mmol) of $FeCl_3 \cdot 6H_2O$ and 3.0 g (15.27mmol) of $FeCl_2 \cdot 4H_2O$ were dissolved in 38 mL of 0.4 M HCl. Afterward, 375 mL of 0.7 M aqueous NH_4OH (28wt%) was added, then a black solid was appeared, which was then vigorously stirred at room temperature for 30 minutes. The black precipitate was gathered using an external magnet placed beneath the reaction bottle, after which the supernatant was decanted and the precipitate was washed adequately times with deionized water. The deposit was then dispersed in 150 mL of deionized water, and a suspension was prepared by combining 50 mL of this solution with 250 mL of 2-propanol, 11.58 mL of PEG-400(Polyethylene glycol with an average molecular weight of 400), 25 mL of NH_4OH, 50 mL of deionized water, 30 mL of TEOS (Tetraethyl orthosilicate), and 3 mL of N-(2-aminoethyl)-3-aminopropyltrimethoxysilane as a modifier. This mixture underwent ultrasonic treatment for 20 minutes, followed by stirring under an argon atmosphere for 24 hours. The final product was then dried under vacuum. The nitrogen content of the produce was determined to be 1.3% through CHN analysis.

2.3. Synthesis of Schiff base

For the synthesis of the Schiff base, 500 mg of the precipitate from the previous step was combined with 5 mL of salicylaldehyde in 80 mL of ethanol as the solvent, and the mixture was vigorously stirred for 48 hours under reflux conditions. Subsequently, the solid obtained was separated using a magnet, extensively rinsed with acetone and ethanol, and subsequently desiccated under vacuum at room temperature for an extended duration.

2.4. Synthesis of $Ru^{III}(OTf)_2$ Salen modified SiO_2–Fe_3O_4

To immobilize $RuCl_3$ onto the magnetic Schiff base nanoparticles, 250 mg of $RuCl_3$ and 500 mg of the precipitate from the previous step were stirred with 20 mg of sodium acetate in 100 mL of acetonitrile for 48 hours under reflux conditions. The resulting precipitate was collected using an external magnet, washed three times with ethanol, and dried under vacuum.

In the final stage, the precipitate from the previous step was stirred with 0.6mmol of NaOTf to replace the Cl^- ligand with OTf^- in 20 mL of THF solvent at a temperature of 60 degrees Celsius for one hour. The resulting precipitate was then washed multiple times with acetone and dried at room temperature (Fig. 1).

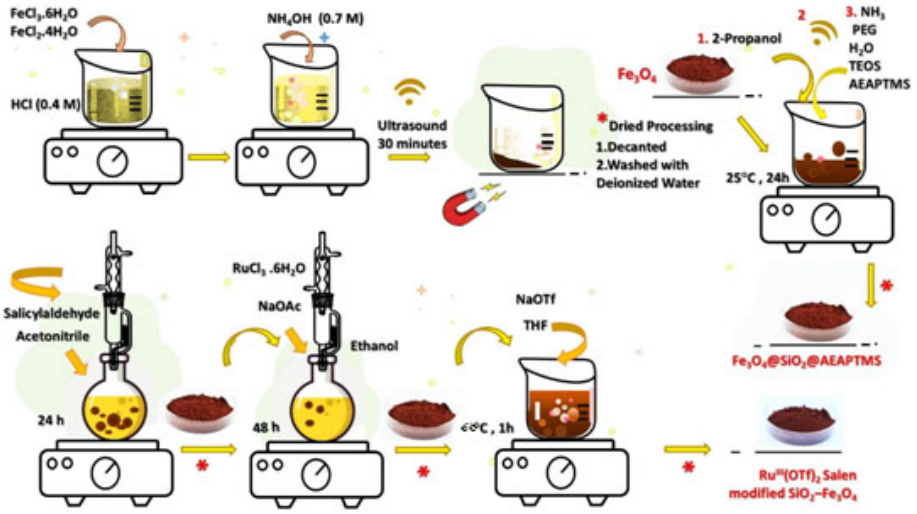

Fig. 1. Scheme of synthesis $Ru^{III}(OTf)_2$ Salen modified SiO_2–Fe_3O_4

3. Analysis of the characteristics of immobilized $Ru^{III}(OTf)_2$ Salen modified SiO_2–Fe_3O_4

3.1. Characterization of the catalyst

3.1.1. XRD analysis

The procedure for modifying the silica shell on magnetic nanoparticles with N-(2-aminoethyl)-3-aminopropyltrimethoxysilane (AEAPTMS) to produce NH_2SiO_2–Fe_3O_4 was carried out in accordance with the method outlined by McKittrick and Jones. The nitrogen content in NH_2SiO_2–Fe, as determined through CHN analysis (Carbon, Hydrogen, and Nitrogen elemental analysis), was approximately 1.3 $mmol.g^{-1}$. Furthermore, the examination of the ruthenium content in the supported catalyst using ICP (Inductively Coupled Plasma) revealed a concentration of 0.5 $mmol.g^{-1}$ of the supported catalyst. X-ray Diffraction (XRD) patterns were obtained from the synthesized nanoparticles to confirm that they were Fe_3O_4 and not Fe_2O_3. Figure 2 depicts the XRD patterns of the Fe_3O_4 magnetic nanoparticles (MNPs), which closely match the crystal structure pattern of magnetite. The distinctive

peaks are observed at 2θ positions = 18.27° (111), 30.04° (220), 37.05° (311), 43.05° (400), 53.39° (422), 56.94° (511), 62.52° (440) [31].

The presence of $Ru^{III}(Salen)OTf_2$ on the support was further confirmed by the UV–visible spectrum. The diffuse reflectance spectrum of the supported catalyst matrix exhibited two bands at 360 nm, which are characteristic of the d–d transitions of the Ru(III) Salen complex (Fig. 3).

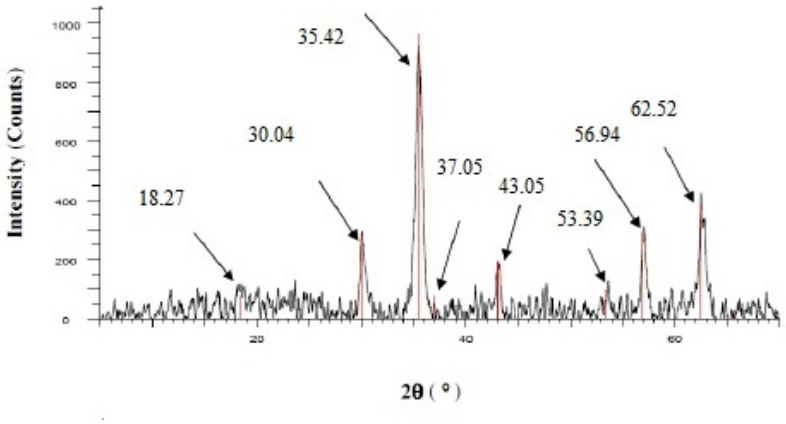

Fig. 2. XRD pattern related to Fe_3O_4

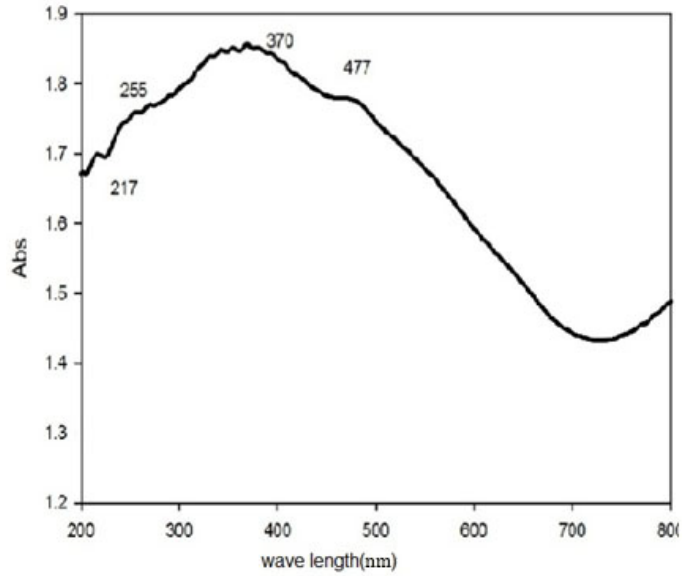

Fig. 3. UV-Vis spectrum related to $Ru^{III}(OTf)_2$ Salen modified SiO_2–Fe_3O_4

3.1.2. FT-IR analysis

In the FT-IR spectra of the MNPs (Fig. 4) there are a Fe-O stretching vibration at around 593 cm^{-1}, that's indicates the presence of iron oxide. Moreover, the modified nanoparticles showed an OH-stretching vibration nearby 3434 cm^{-1}, relevant to physisorbed water and possible surface hydroxyl groups. Peaks about 1038 cm^{-1} were also observed, corresponding to Si-O stretching vibrations. Likewise, the immobilized ligand and catalyst showed peaks near 2811 cm^{-1} and 2941 cm^{-1}, which are related $–CH_2$ vibrations. The clear band at 1616 cm^{-1} was attributed to the -C=N stretching vibration of the imine group of the ligand, indicating the effective organization of the Schiff base [32].

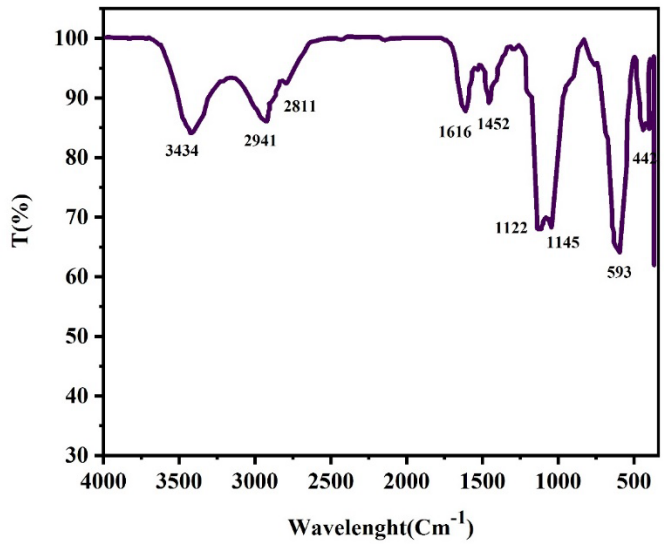

Fig. 4: FT-IR spectrum related to $Ru^{III}(OTf)_2$ Salen modifed SiO_2–Fe_3O_4

3.1.3. SEM and EDX analysis

The shape and size of the MNPs were captured by scanning electron microscopy (SEM). The SEM pictures showed that MNPs have a uniform morphology and consist of spherical particles with an average size of 27 nm. The particles were evenly dispersed and did not exhibit substantial agglomeration, as showed in Fig. 5.

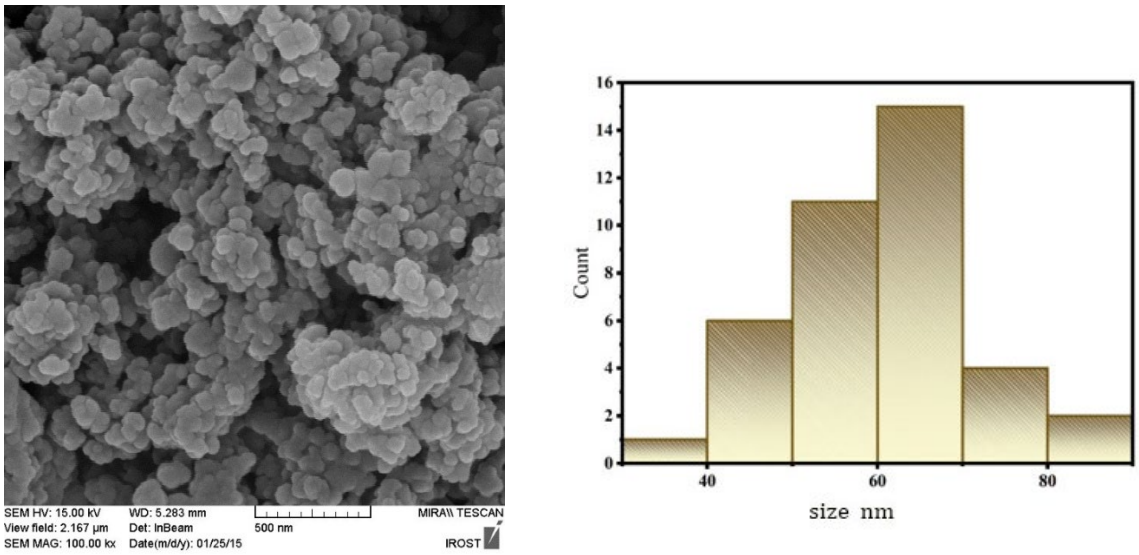

Fig. 5. SEM images of a$Ru^{III}(OTf)_2$ Salen modified SiO_2–Fe_3O_4 nanoparticles b) histogram related to SEM image of Ru^{III}(OTf)2 Salen modifed SiO_2–Fe_3O_4 nanoparticles

Furthermore, the results from energy dispersive X-ray (EDX) analysis illustrated that the Fe_3O_4_SiO_2/AEAPTMS/Salen/$Ru(OTf)_2$ nanoparticles (Fig. 6) contain numerous elements, including Fe, O, Si, N, C, Ru, and F.

3.1.4. VSM analysis

The VSM analysis showed that these nanoparticles have a high saturation magnetization as determined from the magnetization curves (Fig. 7), which measures their maximum magnetic strength. The saturation magnetization values were found to be 69.4845 emu/g for Fe_3O_4, 43.4457 emu/g for Fe_3O_4_SiO_2, and 37.5647 emu/g for

Fe_3O_4_SiO_2/AEAPTMS/Salen/Ru $(OTf)_2$ nanoparticles. Even though the reduction in saturation magnetization owing to silica coating, the nanoparticles engaged sufficient levels of magnetization for magnetic separation using a usual magnet. The lack of a hysteresis loop in the magnetization curve confirmed that the synthesized Fe_3O_4_SiO_2/AEAPTMS/Salen/Ru $(OTf)_2$ nanoparticles were superparamagnetic and could be simply separated from the mixture with an external magnetic field.

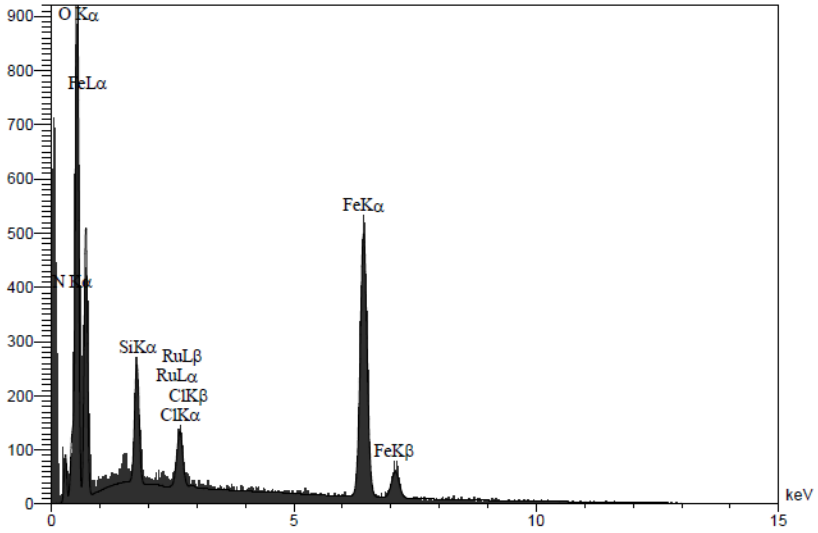

Fig. 6. The results of EDX analysis of Fe_3O_4_SiO_2/AEPTMS/Salen Ru$(OTf)_2$ catalyst nanoparticles

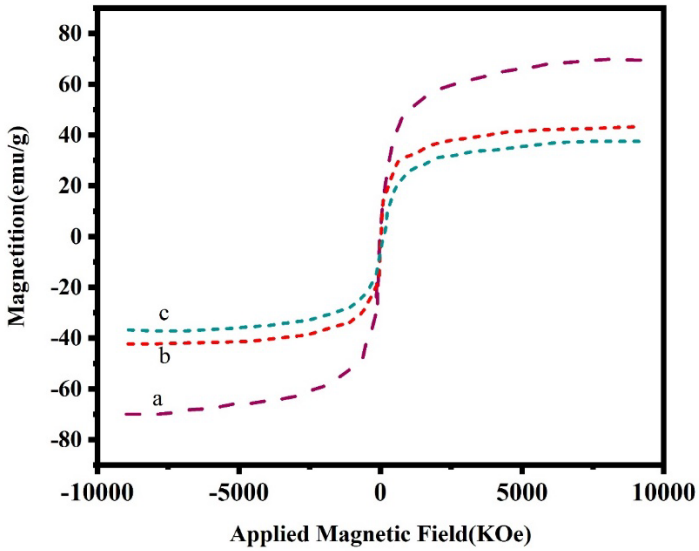

Fig. 7. VSM diagrams related to a) Fe_3O_4 b) Fe_3O_4_SiO_2 c) $Ru^{III}(OTf)_2$ Salen modified SiO_2–Fe_3O_4

3.2. Catalyst study

3.2.1. General process for acetylation of alcohol and phenols with Ac_2O catalyzed by $Ru^{III}(OTf)_2$ Salen modified SiO_2–Fe_3O_4

In general, at ambient temperature, the mixture of alcohol or phenol (1 mmol) and Ac_2O (3 mmol per OH group) in CH_3CN as solvent (1 mL) and catalyst for 0.01 mmol (0230 mg) was mixed. The evolution of the reaction completion was monitored by gas chromatography. After achievement of the reaction, the solvent was evaporated, 10 mL of Et_2O

was added, and the catalyst was recovered using an external magnet. The filtrates were washed with brine, dried over Na_2SO_4, and concentrated under reduced pressure to afford the crude product.

3.2.2. Optimization of reaction conditions

This study considered the catalytic presentation of $Ru^{III}(OTf)_2$Salen modified SiO_2–Fe_3O_4 in the acetylation of benzyl alcohol with acetic anhydride. Optimization of reaction conditions, involving catalyst amount and solvent selection, was survived. The highest yield was achieved with 230 mg of Ru catalyst in the typical reaction. Among of several solvents, such as CH_2Cl_2, CH_3CN, EtOAc, n-hexane, and chloroform, revealed that CH_3CN supplied the highest yield. Subsequently, CH_3CN was selected as the solvent for the reaction.

In the initial step of our study, a model reaction was managed using 4-chlorobenzyl alcohol (1.0 mmol) and acetic anhydride (3.0 mmol) to assess the efficiency of $Ru^{III}(OTf)_2$ Salen modifed SiO_2–Fe_3O_4 catalyst (230 mg) in several solvents (Table 1). The results showed that CH_3CN was the most effectual and fastest solvent for the acetylation of alcohols (Table 1, entry 3).

Table 1. The impact of solvents on the acetylation of alcohols and phenols with acetic anhydride in the presence of a $Ru^{III}(OTf)_2$ Salen modifed SiO_2–Fe_3O_4

Entry	Solvent	Yield(%)[b]
1	CH_2Cl_2	75
2	$CHCl_3$	64
3	CH_3CN	93
4	THF	27
5	CH_3COCH_3	61

a) Reaction conditions: 4-chlorobenzyl alcohol (1mmol), acetic anhydride (3mmol), catalyst (230mg), and solvent (1mL) were reacted for 3 minutes.

b) The yield was determined by GC analysis based on 4-chlorobenzyl alcohol.

The mass of catalyst was also weighed, and it was observed that the reaction did not yield significantly in the absence of catalyst (Table 2, entry 1). The highest yield was gotten with 230 mg of Nano catalyst after 3 minutes (Table 2, entry 5). Further increasing the catalyst amount did not lead to a noteworthy improvement in the yield (Table 2, entry 6).

Table 2. The effect of the amount of the Catalyst on the acetylation of alcohols and phenols with acetic anhydride in the presence of a $Ru^{III}(OTf)_2$ Salen modifed SiO_2–Fe_3O_4

Entry	Catalyst mg(mmol)[a]	Yield (%)[b]
1	0(0.000)	5
2	45(0.0214)	57
3	75(0.03)	72
4	100(0.04)	88
5	230(0.01)	93
6	250(0.011)	93

a) Reaction conditions: 4-chlorobenzyl alcohol (1mmol), acetic anhydride (3mmol), catalyst, and CH_3CN (1 mL) for a duration of 3 minutes.

b) The yield was determined by GC analysis based on 4-chlorobenzyl alcohol.

Presenting the acetic anhydride amount to 3mmol in the identical reaction yielded the highest acetate production when 4mmol of acetic anhydride was used (refer to Table 3, entry 2). Consequently, the best outcomes were achieved

when employing 230 mg of the Nano catalyst in the presence of 3mmol acetic anhydride within 1 ml CH_3CN at room temperature.

Table 3. The effect of the amount of acetic anhydride on the acetylation of alcohols and phenols in the presence of $Ru^{III}(OTf)_2$Salen modifedSiO_2–Fe_3O_4 catalyst

Entry	Acetic anhydride (mmol)[a]	Yield (%)[b]
1	1	34
2	2	63
3	2.5	90
4	3	93
5	3.5	93

a) Reaction conditions: 4-chlorobenzyl alcohol (1mmol), catalyst, and CH_3CN (1 mL) for a duration of 3 minutes

b) The yield was determined by GC analysis based on 4-chlorobenzyl alcohol

With these optimized conditions under consideration, a general variety of alcohols, including primary (both benzylic and linear) and secondary alcohols, were effectually acetylated with acetic anhydride in the presence of a catalyst. For benzylic alcohols, those with electron-withdrawing substituents needed greater reaction times to reach completion, whereas those with electron-donating substituents were achieved in shorter time frames (Table 4).

Table 4. Acetylation of alcohols and phenols with acetic anhydride catalyzed by $Ru^{III}(OTf)_2$ Salen modified SiO_2–Fe_3O_4 at room temperature

Entry	Hydroxyl compound	Acetylated compound	Time	Yield (%)	TOF(h^{-1})
1	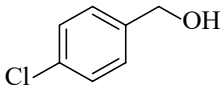	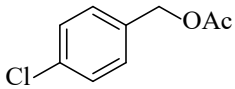	3	93	186
2	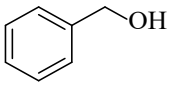	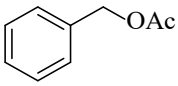	3	92	182
3	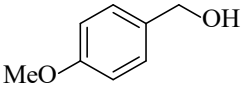	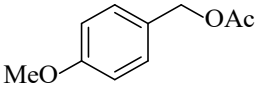	3	93	186
4	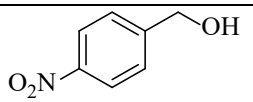	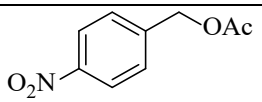	7	90	72
5	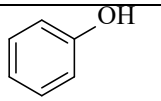	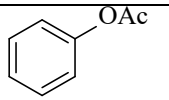	5	87	87
6	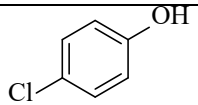	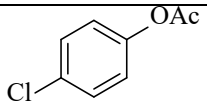	5	87	88
7	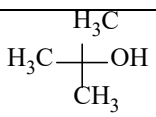	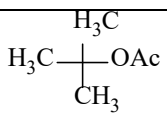	7	80	72
8	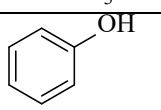	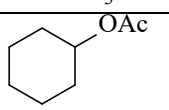	7	87	74
9	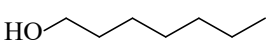	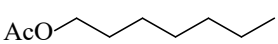	9	87	58

a) Reaction conditions: alcohol or phenol (1mmol), acetic anhydride (3mmol), catalyst (230 mg, 0.1mmol), CH_3CN (1ml).

b) GC yield

c) Reaction was performed with 3mmol of acetic anhydride per OH group

At present, the exact mechanism of the process is not completely understood. Though one possible description is that the catalyst first activates acetic anhydride to form intermediate 1. This intermediate is then attacked by alcohol or phenol, resulting in the formation of the final product and the regeneration of the catalyst for other catalytic cycles (Fig. 8).

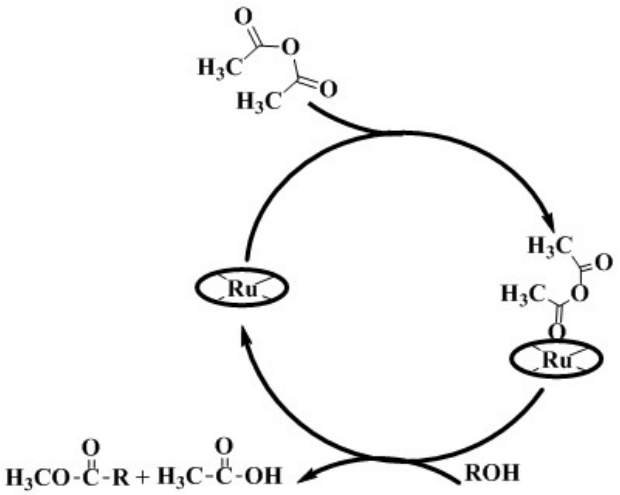

Fig. 8. Proposal mechanism for acetylation of alcohol with $Ru^{III}(OTf)_2$ Salen modified SiO_2–Fe_3O_4

3.3. Catalyst recyclability

The study evaluated the reusability of the catalyst by conducting investigates using 4-chlorobenzyl alcohol as a model compound. The procedure involved using an external magnet to separate the catalyst from the reaction mixture, followed by rinsing the solid twice with 1, 2-dichloroethane. The catalyst was then employed in subsequent runs with a fresh substrate dissolved in the same solvent. The results showed that the catalyst could be reused for several consecutive cycles without experiencing a significant decline in its catalytic effectiveness. This finding highlights the potential for repetitive use of the catalyst, which could lead to cost savings and reduced environmental impact of the reaction. Fig. 9 presents a graph illustrating the minimal decrease in efficiency over ten cycles, demonstrating only a slight reduction in efficiency.

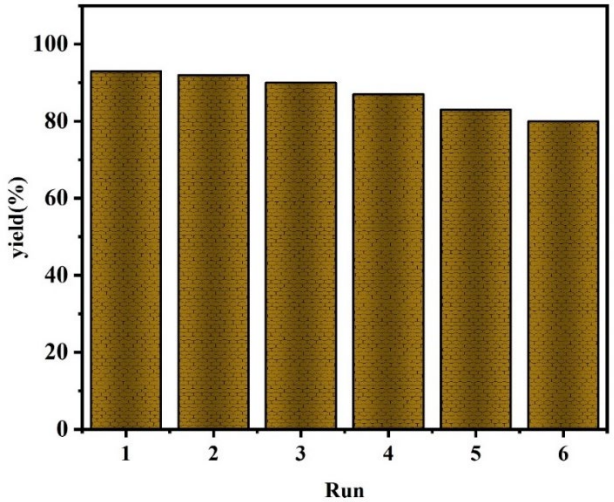

Fig. 9. Diagram of correlation between catalyst recovery cycles and product efficiency

Table 5. Comparison of the effectiveness of $Ru^{III}(OTf)_2$ Salen modifed SiO_2–Fe_3O_4 with other catalysts for the acetylation

Entry	Time (min)	Conversion (%)	Ref.
$ZnAl_2O_4$	18	100	13
P(4-VPH)ClO_4	22	96	14
$ZnAl_2O_4$@SiO_2	20	92	15
5%MoO_3–SiO_2	30	86	16

4. Conclusion

For the acetylation of alcohols and phenols under mild conditions. The catalyst exhibited excellent activity, providing 87–93% yield within 3–9 minutes, and could be easily separated and reused for multiple cycles without significant loss of performance. Comprehensive characterization using FT-IR, XRD, SEM, EDX, and VSM confirmed the successful immobilization and superparamagnetic properties of the catalyst. In addition, FE-SEM (discussed in the Results and Discussion section) revealed the uniform morphology and homogeneous elemental distribution of the catalyst. These results highlight the potential of this Nano catalyst for green and sustainable organic synthesis. Further studies could explore the application of this catalyst in other protection reactions or in continuous-flow systems. Moreover, optimizing the catalyst structure or exploring alternative supports may further enhance its performance and broaden its industrial applicability.

References

[1] Wuts, P.G., Greene, T.W., 2006. Greene's protective groups in organic synthesis. John Wiley & Sons.
[2] Arnodo, D., De Nardo, E., Ghinato, S., Baldino, S., Blangetti, M., Prandi, C., 2023. A mild, efficient and sustainable tetrahydropyranylation of alcohols promoted by acidic natural deep eutectic solvents. ChemSusChem, 16(3), e202202066. https://doi.org/10.1002/cssc.202202066
[3] Rahmanzadeh, A., Daneshvar, N., Shirini, F., Tajik, H., 2021. Comparison of the efficiency of two dicationic ionic liquids catalysts based on perchloric acid for the protection of alcohols. Journal of the Iranian Chemical Society, 18(12), 3295–3302. https://doi.org/10.1007/s13738-021-02267-z
[4] Mehdigholami, S., Koohestanian, E., 2024. Protection of hydroxy groups as trimethylsilyl ethers catalyzed by recyclable magnetically Schiff-base complexes of ruthenium using HMDS. Chemical and Process Engineering: New Frontiers, 45(1), 52. https://doi.org/10.24425/cpe.2023.147411
[5] Mehdigholami, S., Koohestanian, E., 2023. Fe3O4@SiO2/AEPTMS/Fe(OTf)3: An efficient superparamagnetic nanocatalyst for the protecting of alcohols. Journal of Particle Science and Technology, 9(1), 1–9. https://doi.org/10.22104/jpst.2023.6188.1224
[6] Rahmatpour, A., Alinejad, S., Donyapeyma, G., 2022. Noncross-linked polystyrene nanoencapsulation of ferric chloride: A novel and reusable heterogeneous macromolecular Lewis acid catalyst toward selective acetylation of alcohols, phenols, amines, and thiols. Journal of Organometallic Chemistry, 961, 122264. https://doi.org/10.1016/j.jorganchem.2022.122264
[7] Barot, Y., Mishra, S., Anand, V., Mishra, R., 2023. Iron containing di-cationic ionic liquid [DIL]2+[2FeCl4]2− as a highly efficient catalyst for the acylation of alcohols, phenols and amines. Catalysis Communications, 182, 106739. https://doi.org/10.1016/j.catcom.2023.106739
[8] Ghosh, S., Purkait, A., Jana, C.K., 2020. Environmentally benign decarboxylative N-, O-, and S-acetylations and acylations. Green Chemistry, 22(24), 8721–8727. https://doi.org/10.1039/D0GC03731A
[9] Patil, S.M., Ingale, A.P., Pise, A.S., Bhondave, R.S., 2022. Novel cobalt-supported silica-coated ferrite nanoparticles applicable for acylation of amine, phenol, and thiols derivatives under solvent-free condition. ChemistrySelect, 7(26), e202201590. https://doi.org/10.1002/slct.202201590
[10] Chia, P.W., Chee, P.S., Mazlan, N.W., Yong, F.S.J., Rozaini, M.Z.H., Kan, S.Y., 2020. Acetylation of alcohols and amines catalyzed by onion peel ash under a base- and solvent-free condition. Songklanakarin Journal of Science and Technology, 42, 602–607. https://doi.org/10.14456/sjst-psu.2020.76
[11] Kalla, R.M.N., Chakali, R., Raju, C.N., 2024. Protection of aldehydes and hydroxy compounds with acetic anhydride in the presence of sulfonic acid functionalized ionic liquid. Organic Communications, 17(1), 1–7. https://doi.org/10.25135/acg.oc.161.2312.2995
[12] Dey, A.K., Majhi, S., 2023. Samarium(III) triflate in organic synthesis: a mild and efficient catalyst. Chemistry Select, 8(18), 202300156. https://doi.org/10.1002/slct.202300156
[13] Farhadi, S., Panahandehjoo, S., 2010. Spinel-type zinc aluminate (ZnAl2O4) nanoparticles prepared by the co-precipitation method: A novel, green and recyclable heterogeneous catalyst for the acetylation of amines, alcohols and phenols under solvent-free conditions. Applied Catalysis A: General, 382(2), 293–302. https://doi.org/10.1016/j.apcata.2010.05.005

[14] Khaligh, N.G., 2012. Preparation, characterization and use of poly(4-vinylpyridinium) perchlorate as a new, efficient, and versatile solid-phase catalyst for acetylation of alcohols, phenols and amines. Journal of Molecular Catalysis A: Chemical, 363, 90–100. https://doi.org/10.1016/j.molcata.2012.05.021
[15] Farhadi, S., Jahanara, K., 2014. ZnAl2O4@SiO2 nanocomposite catalyst for the acetylation of alcohols, phenols and amines with acetic anhydride under solvent-free conditions. Chinese Journal of Catalysis, 35(3), 368–375. https://doi.org/10.1016/S1872-2067(12)60758-X
[16] Hlatshwayo, X.S., Ndolomingo, M.J., Bingwa, N., Meijboom, R., 2021. Molybdenum-modified mesoporous SiO2 as an efficient Lewis acid catalyst for the acetylation of alcohols. RSC Advances, 11(27), 16468–16477. https://doi.org/10.1039/D1RA02134F
[17] Raczuk, E., Dmochowska, B., Samaszko-Fiertek, J., Madaj, J., 2022. Different Schiff bases—structure, importance and classification. Molecules, 27(3), 787. https://doi.org/10.3390/molecules27030787
[18] Whiteoak, C.J., Salassa, G., Kleij, A.W., 2012. Recent advances with π-conjugated salen systems. Chemical Society Reviews, 41(2), 622–631. https://doi.org/10.1039/C1CS15170C
[19] Kumagai, Y., Takabe, R., Nakazono, T., Shoji, M., Isobe, H., Yamaguchi, K., Wada, T., 2024. Water oxidation utilizing a ruthenium complex featuring a phenolic moiety inspired by the oxygen-evolving centre (OEC) of photosystem II. Sustainable Energy & Fuels, 8(5), 905–913. https://doi.org/10.1039/D3SE01610B
[20] Bühler, J., Muntwyler, A., Roithmeyer, H., Adams, P., Besmer, M.L., Blacque, O., Tilley, S.D., 2024. Immobilised ruthenium complexes for the electrooxidation of 5-hydroxymethylfurfural. Chemistry – A European Journal, 30(19), e202304181. https://doi.org/10.1002/chem.202304181
[21] Xu, Z.C., Ma, X.R., Zhang, L.J., Chen, H.T., Qing, D.M., Li, R.T., Wang, R.R., 2024. Antifungal activity of ruthenium(II) complex combined with fluconazole against drug-resistant Candida albicans in vitro and its anti-invasive infection in vivo. Journal of Inorganic Biochemistry, 255, 112522. https://doi.org/10.1016/j.jinorgbio.2024.112522
[22] Halder, S., Naskar, S., Jana, D., Kanrar, G., Pramanik, K., Ganguly, S., 2024. Ruthenium complexes of redox non-innocent aryl-azo-oximes for catalytic α-alkylation of ketones and synthesis of 2-substituted quinolines. New Journal of Chemistry, 48(18), 8181–8194. https://doi.org/10.1039/D4NJ00391H
[23] Morozkov, G.V., Abel, A.S., Lyssenko, K.A., Roznyatovsky, V.A., Averin, A.D., Beletskaya, I.P., Bessmertnykh-Lemeune, A., 2024. Ruthenium(II) complexes with phosphonate-substituted phenanthroline ligands as reusable photoredox catalysts. Dalton Transactions, 53(2), 535–551. https://doi.org/10.1039/D3DT02936K
[24] Azadi, S., Sardarian, A.R., Esmaeilpour, M., 2023. Nano Cr(III) Schiff-base complex supported on magnetic Fe3O4@SiO2: Efficient, heterogeneous, and recoverable nanocatalyst for chemoselective synthesis of 1,2-disubstituted benzimidazoles. Monatshefte für Chemie – Chemical Monthly, 154(8), 887–903. https://doi.org/10.1007/s00706-023-03100-4
[25] Azadi, S., Sardarian, A.R., Esmaeilpour, M., 2021. Magnetically recoverable Schiff base complex of Pd(II) immobilized on Fe3O4@SiO2 nanoparticles: An efficient catalyst for the reduction of aromatic nitro compounds to aniline derivatives. Monatshefte für Chemie – Chemical Monthly, 152(7), 809–821. https://doi.org/10.1007/s00706-021-02787-7
[26] Kalhor, M., Banibairami, S., Mirshokraie, S.A., 2018. Ni@zeolite-Y nanoporous: A valuable and efficient nanocatalyst for the synthesis of N-benzimidazole-1,3-thiazolidinones. Green Chemistry Letters and Reviews, 11(3), 334–344. https://doi.org/10.1080/17518253.2018.1499968
[27] Somwanshi, S.B., Somvanshi, S.B., Kharat, P.B., 2020. Nanocatalyst: A brief review on synthesis to applications. Journal of Physics: Conference Series, 1644(1), 012046. https://doi.org/10.1088/1742-6596/1644/1/012046
[28] Koohestanian, E., Mehdigholami, S., 2023. Synthesis of hematite nanoparticles by ball milling and the study of their magnetic properties and microstructure. Chemical Process Design, 2(2), 52–59. https://doi.org/10.22111/cpd.2024.47291.1030
[29] Veisi, H., Pirhayati, M., Mohammadi, P., Tamoradi, T., Hemmati, S., Karmakar, B., 2023. Recent advances in the application of magnetic nanocatalysts in multicomponent reactions. RSC Advances, 13(30), 20530–20556. https://doi.org/10.1039/D3RA01208E
[30] McKittrick, M.W., Jones, C.W., 2003. Toward single-site functional materials: Preparation of amine-functionalized surfaces exhibiting site-isolated behavior. Chemistry of Materials, 15(5), 1132–1139. https://doi.org/10.1021/cm020952z
[31] Dawn, R., et al., 2022. Origin of magnetization in silica-coated Fe3O4 nanoparticles revealed by soft X-ray magnetic circular dichroism. Brazilian Journal of Physics, 52(3), 99. https://doi.org/10.1007/s13538-022-01102-x
[32] Azadi, S., et al., 2024. Antifungal activity of Cu(II) magnetic nanoparticles against pathogenic Candida species. Scientific Reports, 1–13. https://doi.org/10.1038/s41598-024-56512-5
[33] Gonzalez-Carrillo, G., Gonzalez, J., Emparan-Legaspi, M.J., Lino-Lopez, G.J., Aguayo-Villarreal, I.A., Ceballos-Magaña, S.G., Muñiz-Valencia, R., 2020. Propylsulfonic acid grafted on mesoporous siliceous FDU-5 material: A high TOF catalyst for the synthesis of coumarins via Pechmann condensation. Microporous and Mesoporous Materials, 307, 110458. https://doi.org/10.1016/j.micromeso.2020.110458